Fazl Ali College Journal, ISSN:2319-6769, Vol. 7 (2017) 120 - 127

Probing the Magnetic Transitions in Europium Chromite through Electron Paramagnetic Resonance

Oimang Borang[1], S.Srinath[2], S. N. Kaul[2], and Y. Sundarayya[2] *

1 Department of Physics, School of Sciences, Nagaland University, Lumami - 798627, Nagaland, India.
2 School of Physics, University of Hyderabad, Prof. C. R. Rao Road, Gachibowli, Hyderabad - 500 046, A.P, India.

Received : 27 October 2017

Abstract

We report the synthesis of homogeneous single phase $EuCrO_3$ nanoparticles by a modified sol-gel followed by hydrothermal methods. Annealing the as-synthesized amorphous powder at 973 K and ambient pressure reveals $EuCrO_3$ crystallizes into orthorhombic perovskite structure with space group *Pbnm* and D_{4h}^{19} symmetry. DC magnetic measurements suggest that the Cr^{3+} spins undergo a paramagnetic – antiferromagnetic transition with canting of spins at Cr sublattices with Néel temperature, $T_N = 181K$, as a consequence of antisymmetric Dzyaloshinsky-Moriya (DM) Cr–O–Cr super exchange interaction. Analysis of temperature-dependent electron paramagnetic resonance spectra reveals that the line-width (ΔH_{pp}), the differential intensity (ΔI_{pp}), the spontaneous magnetization ($4\pi M_S$) and the magnetic anisotropy field (H_k) show an abrupt transition at Néel temperature.

Key words: Sol-gel processing, Nanocrystalline materials, Antiferromagnetics.
PACS: 81.20.Fw, 73.63.Bd, 75.50.Ee

Introduction

Magnetoelectric multiferroics constitute a class of novel materials in which interaction between coupled electric and magnetic dipoles (with two order parameters) leads to magnetoelectric effect **[1–5]**. Rare-earth orthochromites, $RCrO_3$ (R = rare earth/ Yttrium), isostructural orthoferrites, $RFeO_3$ are such class of oxides that got the attention of researchers due to their electronic correlations with unusual magnetoelectric properties **[6–9]**. They are of great interest notably due to the observed high coercive fields when deposited in the form of thin films **[10]**. $RCrO_3$ compounds crystallize into orthorhombic perovskite structure (Space group *Pbnm* and D_{4h}^{19}crystal symmetry) with a nine-coordinated A-site, occupied by the rare-earth ion, R^{3+} ($4f^{1\text{-}14}$), while the chromium ion, Cr^{3+} ($4s^0 3d^3$) is at octahedral B-site. The Cr^{3+} spins at the chromium sublattice undergo a paramagnetic (PM) to antiferromagnetic (AFM) transition with a canting of spins at Cr sites **[11, 12]**. This is due to antisymmetric Dzyaloshinskii-Moriya (DM) exchange interaction between neighboring Cr^{3+} spins that leads to weak ferromagnetism with $\Gamma_4(G_x,$

* Corresponding author: ysundar@nagalanduniversity.ac.in

A_y, F_z) spin structure, as reported in $YCrO_3$**[13–15]**. However, the ground state configuration, Γ_4 remains the same unless affected by the presence of magneto-crystalline anisotropy. The presence of a magnetic R^{3+} ion (in place of non-magnetic Y^{3+}) brings in magnetic anisotropy that promotes phenomena like negative magnetization, magnetic compensation and spin-reorientation (SR) in $RCrO_3$**[16, 17]**. This temperature-dependent 3*d*-4*f* interaction between magnetic R^{3+} and Cr^{3+} may give rise to $\Gamma_2(F_x, C_y, G_z)$ and/or $\Gamma_1(A_x, G_y, C_z)$ ground state spin configurations with Γ_1 being the collinear antiferromagnetic spin structure of Cr sublattice. Since the magnetism due to R^{3+} is masked by Cr^{3+} over a wide range down to low temperatures, limited is known about the magnetic anisotropy of the rare-earth in $RCrO_3$ oxides [**18, 19]**. In particular, the population of non-magnetic ground term $^7F_0$ of Eu^{3+} makes the anisotropy of paramagnetic Eu^{3+} to be minimal in $EuCrO_3$. This may lead to the dominant magnetic behavior by Cr^{3+} at low temperatures resulting in $\Gamma_2(F_x, C_y, G_z)$ configuration**[20–22]**. Similar observation may be made in $SmCrO_3$. The presence of a strong anisotropic rare-earth leads to collinear $\Gamma_1(A_x, G_y, C_z)$ configuration in $ErCrO_3$.This necessitates studying the complex magnetic behavior of $RCrO_3$. In view of such exciting magnetic behavior, we report the synthesis of homogeneous single phase $EuCrO_3$ through a modified sol-gel route with hydrothermal method followed by magnetic properties through DC magnetization measurements and temperature-dependent electron paramagnetic resonance (EPR) spectra of $EuCrO_3$.

Experimental Section

Homogeneous single phase $EuCrO_3$ nanoparticles have been synthesized through a modified sol-gel method followed by hydrothermal procedure and annealing treatment. The detailed synthesis technique adopted was given elsewhere **[23, 24]**. The as-synthesized sample was characterized by X-ray powder diffraction (XRD) using Bruker D8 Advance diffractometer with Cu-Kα radiation (λ = 1.54056 Å). DC Magnetic measurements were carried out with a vibrating sample magnetometer in a Physical Property Measurement System (PPMS). Temperature dependent electron paramagnetic resonance (EPR) spectra were recorded in the X-band region on JEOL-FE3X ESR spectrometer in the range 118 – 373 K, using a liquid nitrogen (LN2) cryostat.

Results and Discussion

The X-ray diffractogram of the as synthesized sample with Rietveld profile matching is shown in figure 1. It confirms that $EuCrO_3$ crystallizes into orthorhombic structure with space group *Pbnm*. The obtained lattice parameters are a = 5.5177 (1) Å, b = 7.6328 (1) Å and c = 5.3472 (1) Å. The average crystallite size, t, has been estimated by Scherer's formula **[25]**

$$t = \frac{0.94\lambda}{B\cos\theta_B} \qquad \text{——} \quad (1)$$

The obtained value of average crystallite size of $EuCrO_3$ is 40 (2) nm. Figure 2 shows the zero-field-cooled (ZFC) and field-cooled (FC) magnetization measurements on $EuCrO_3$ nanoparticles in the temperature range 3 K ≤ T ≤ 350 K. The ZFC and FC measurements were carried out in the presence of an external magnetic field, H = 100 Oe. It reveals the FC-magnetization of $EuCrO_3$ increases with a decrease in temperature at ~ 181 K indicating the PM to canted AFM transition, marked as Neél temperature, T_N, due to the canting of antiferromagnetically ordered spins at Cr sublattices as a result of antisymmetric Dzyaloshinskii – Moriya interaction. The observed value of T_N for $EuCrO_3$ matches with the literature and confirms size effects do not play a role in altering the transition temperature **[26]**. The FC-magnetization increases further below T_N before a decrease is observed below 60 K. This temperature is marked as spin-reorientation

temperature, T_{SR}. This could be due to fact that the Cr^{3+} spins in the canted antiferromagnetic chromium sublattice are getting reoriented to collinear antiferromagnetic spin structure. However, the non-zero magnetization (0.34 emu/g) observed at T = 3.5 K indicates the ground state spin structure is Γ_2 and rules out the presence of Γ_1 structure in $EuCrO_3$. This is due to the anisotropy of the Europium sub-lattice over the chromium sub-lattice, and is expected in orthochromites **[16, 17]**. The inset of figure 2 shows the inverse susceptibility (χ^{-1}) of $EuCrO_3$ obtained from the FC-magnetization, found to be nonlinear in the paramagnetic regime. The deviation of χ^{-1} of $EuCrO_3$ from Curie-Weiss behavior is due to the spacing of the multiplet levels of Eu^{3+}, dissimilar to kT that makes the some of the Eu^{3+} ions to be excited states, suggested by Van Vleck and Frank **[21, 22]**. Hence the inverse susceptibility has been analyzed by using the modified Curie-Weiss equation given by

$$\chi^{-1} = \left[\left(\frac{C_w}{T-\theta_{cw}}\right) + \chi\right]^{-1} \qquad \text{—— (2)}$$

where $C_w = 0.012895$, is Curie constant and θ_w = +17.03 K, is Curie temperature. The positive value of θ_{CW} for $EuCrO_3$ indicates the dominant WFM interactions over antiferromagnetic interaction with possible existence of $\Gamma_2(F_x, C_y, G_z)$ phase ground state. It immediately follows that chromium ions do not exist in collinear magnetic ground state. The effective magnetic moment of $EuCrO_3$, μ_{eff} is calculated by using the formula, $\mu_{eff} = \left[\frac{3\chi k_B C}{N\mu_\beta^2}\right]^{1/2}$ and found to be 5.1 μ_β. This may be accounted for the magnetic moment of the paramagnetic Eu^{3+} ($\mu_{eff} = 3.48\mu_B$) added to that of residual weak ferromagnetic moment of the canted antiferromagnetically coupled Cr^{3+} ($\mu_{eff} = 3.87\mu_B$) of the Γ_2 structure. It is to be noted that the deviation of the plot of $1/\chi$ from the fit is more apparent above 300 K.

To examine the magnetic transitions, temperature dependent electron paramagnetic resonance spectra (EPR) were recorded on $EuCrO_3$ nanoparticles in the X-band region in the range 118 – 373 K. EPR is a powerful tool to study the dynamics of spin states across the transition in a magnetic system, canted antiferromagnets in particular. Figure 3 shows such as-recorded EPR spectra of $EuCrO_3$ nanoparticles at three different temperatures 118, 273 and 373 K respectively, with rate of power *dP/dH* absorbed on the Y-axis with respect to the external magnetic field H on the X-axis. The EPR spectral parameters obtained from the observed spectral analysis are the resonance field, H_{res} (the field where the dP/dH = 0 line cuts the dP/dH versus H curve), the peak-to-peak width, ΔH_{pp} (the field difference between the extrema of the dP/dH versus H curve), the peak-to-peak differential intensity, ΔI_{pp} (the spectral intensity difference between the extrema of dP/dH versus H curve).

Figures 4(a) shows the variation of observed values of ΔI_{pp} as a function of temperature. It reveals that the values of ΔI_{pp} are nearly constant from 118 K to 178 K. Further increase in temperature results an abrupt increase in ΔI_{pp} values in the temperature range 178 – 188 K, depicts a magnetic transition. Above 188 K, the ΔI_{pp} values decrease gradually up to 372 K with a dip around 293 K. Figures 4(b) shows the variation of observed values of ΔH_{pp} as a function of temperature. It reveals that the values of ΔH_{pp} do not vary appreciably from 118 K to 178 K. A sudden increase in ΔH_{pp} values has been observed at temperature 178 K, corroborated by a magnetic transition with an abrupt change of ΔI_{pp} values. This is attributed to canted antiferromagnetic to paramagnetic transition of the Cr^{3+} spin structure in $EuCrO_3$ with Néel temperature, T_N = 181 K, observed from DC magnetic measurements. Further increase in temperature results a gradual increase of ΔH_{pp} values from 183 – 297 K. Further, an abrupt

decrease of the ΔH_{pp} values has been observed from 297 – 312 K; similar to a dip in ΔI_{pp} values around 293 K, indicates the presence of a magnetic transition in $EuCrO_3$.

To ascertain the nature of magnetic anisotropy of europium on the chromium sublattice, the EPR spectra have been analyzed by lineshape analysis **[27, 28]**. The complete lineshape of dP/dH versus H curves recorded at different temperatures on $EuCrO_3$ have been analyzed with the aid of a non-linear least square fit program in the light of Landau-Lifshitz-Gilbert (LLG) equation for a polycrystalline material. The program treats the Lande's splitting factor g, saturation magnetization M_s as free-fitting parameters and makes use of the observed values of ΔH_{pp} ($1.45\lambda\omega/\gamma^2 M_S$). The values of anisotropy field H_k are derived from the lineshape analysis using the resonance condition given by

$$[(\omega/\gamma)^2 + \Gamma^2] = (H_{res} + 4\pi M_S + H_k)(H + H_k) \quad \text{—— (3)}$$

where $\Gamma = \lambda\omega/\gamma^2 M_S$, $\gamma = ge/2mc$,magneto-mechanical ratio and λ is the Gilbert damping factor. In addition, the lineshape analysis reveals that the Lande's splitting factor *g* has a temperature-independent value of about 2.00 throughout the temperature range, which resembles the paramagnetic nature of the $EuCrO_3$. This is due to the fact that $EuCrO_3$ contains two magnetic viz. Eu^{3+} and Cr^{3+} species. It is to be noted that Cr^{3+} spins undergo a PM – CAFM transition below Néel temperature, T_N = 190 K, while the Eu^{3+} spins may remain to be paramagnetic down to low temperatures that gives rise to nearly constant value of the Lande's splitting factor.

Figures 5(a) and 5(b) show the variation of spontaneous magnetization, $4\pi M_S$ (emu/cm^3) and magnetic anisotropy field, H_k (kOe) of $EuCrO_3$ in the temperature range 118 – 373 K, obtained from the analysis of temperature dependent EPR spectra using LLG equations. Figure 5(a) reveals that the values $4\pi M_S$ do not vary appreciably in the temperature range 118 – 173 K. The spontaneous magnetization undergoes a rapid decrease from 173 K to 183 K with increasing temperature, indicating the canted antiferromagnetic to paramagnetic transition in $EuCrO_3$. Above 183 K, the $4\pi M_S$ value is nearly constant up to 288 K with a sudden rise in the range 288 – 308 K. In addition, the spontaneous magnetization is constant above 308 K, in the paramagnetic regime. Figure 5(b) demonstrates that the values of magnetic anisotropy field (H_k) are nearly constant in the temperature range 118 – 173 K before the H_k values undergo a rapid decrease in the range 173 – 183 K. Again, the anisotropy field values do not change noticeably in the range 183 – 288 K and undergo a sudden increase in the range 288 – 308 K before the H_k values become nearly constant. A similar trend has been observed in the case of spontaneous magnetization, $4\pi M_S$ values. It should be noted that the variation of $4\pi M_S$ and H_k in the range is attributed to the canted antiferromagnetic – paramagnetic transition of Cr^{3+} spin structure in $EuCrO_3$, supported by the variation of ΔH_{pp} and ΔI_{pp} values. However, the magnetic transition observed in the temperature range 288 – 308 K, supported by the variation of ΔH_{pp}, ΔI_{pp}, $4\pi M_S$ and H_k with the apparent non-linear behavior of inverse susceptibility (χ^{-1}) in the paramagnetic regime of $EuCrO_3$ is not known and needs further investigation.

Conclusions

$EuCrO_3$ nanoparticles have been synthesized by a modified so-gel followed by hydrothermal method and annealing. DC magnetic measurements show the $EuCrO_3$ undergoes a paramagnetic – antiferromagnetic transition at T_N ~ 190 K with canting of spins at chromium sublattice due to antisymmetric Dzyaloshinskii – Moriya transition. At low temperatures, the

chromium spin-structure appears to take $\Gamma_2(F_x, C_y, G_z)$ configuration. Detailed analysis of the temperature dependent EPR spectra recorded in the range 118 – 373 K shows the Eu^{3+} spins remain in the paramagnetic state and the magnetic anisotropy plays a major role in tuning the spin structure of chromium. This is corroborated by an abrupt variation of line-width (ΔH_{pp}) and Differential intensity (ΔI_{pp}), the spontaneous magnetization ($4\pi M_S$) and magnetic anisotropy field (H_k) at Néel temperature.

Reference

1. Dzyaloshinskii I. E. (1960), *Soviet Physics*, **10**, 628.
2. Astrov D. N. (1960), *Soviet Physics*, **11**, 708.
3. Folen V. J. , Rado G. T. and Stalder E. W. (1961), *Phys. Rev. Lett.,* **6**, 607.
4. Astrov D.N. (1961), *Soviet Physics*, **13**, 729.
5. Rado G. T. and Folen V. J. (1961), Phys. Rev. Lett., **7**, 310.
6. White R.L. (1969), *J. Appl. Phys.***40(3)**,1061.
7. Tsymbal L.T. , Bazaliy Y.B., Derkachenko V.N.,.Kamenev V.I , Kakazei G.N., Palamares F.J. and. Wigen P.E (2007), *J. Appl. Phys.*,**101**, 123919.
8. Yamaguch T. (1974), *J. Phys. Chem. Solids*,**35**, 479.
9. Goodenough J. B. (2004), Rep. Prog. Phys. **67**, 1915.
10. Belov K.P., Derkachenko V.N. , Kadomtseva A.M., Ovchinnikova T.L., Timofeeva V.A. and Khokhlov V.A. (1975), *Fiz. Tverd. Tela*,**17**, 3328.
11. Rajeswaran B., Khomskii D.I., Zvezdin A.K., Rao and C.N.R.. Sundaresan A. (2012), *Phys.Rev.*B,**86**, 214409.
12. Zhao H.J., Iniguez J., Chen X.M., and Bellaiche L. (2016), *Phys. Rev*. B, **93**, 014417.
13. Singh I., Nigam A. K.,Katharina Landfester Rafael Munoz-Espi and Chandra A., Appl. (2013), *Phys. Lett*., **103**, 182902.
14. Serrao C.R., Kundu A.K., Krupanidhi S. B., Waghmare U. V., and Rao C.N.R. (2005), *Phys. Rev.* B (Rapid Comm.), **72**, 220101.
15. Alvarez G., Montiel H., Cruz M.P., Duran A.C. and Zamorano R., *Journal of Alloys and Compounds* (2011), **509**, L331.
16. Sakata T., and Enomura A. (1979,) *Phys. Status Solidi* A**52**, 311.
17. Aring K.B., and Sievers A. J. (1970), *J. Appl. Phys.***41**, 1197.
18. Bertaut E. F. (1968) in *Magnetism III*, edited by Rado G. T. and Suhl H. (Academic, New York), p. 149.

19. Bertaut E. F., Bassi G., Buisson G., Burlet P., Chappert J., Delapalme A., Mareschal J., Roult G., Aleonard R., Pouthenet R., and Rebouillat J. P. (1966), *J. Appl. Phys*. **37**, 1038.

20. Morales-Sánchez A., Fernández F. and Sáez-Puche R. (1993), *J. Alloy. Comp.* **201**, 161.

21. Van Vleck J. H. (1965), Theory of Electric and Magnetic Susceptibilities, Oxford University Press:Oxford.

22. Morrish A. H. (2001), *The Physical Principles of Magnetism*, Wiley-IEEE Press:New York.

23. Sundarayya Y., Kaul S.N., and Srinath S. (2015), AIP Conference Proceedings, **1665**, 050126.

24. Jaiswal A., Das R., Vivekanand K., Maity T., Abraham P.M., Adyanthaya S., and Poddar P. (2010), *Journal of Applied Physics*,**107**, 013912.

25. Cullity B. D. (1978), *Elements of X-ray diffraction* (Addison-Wesley, Massachusetts) .

26. Taheri M., Razavi F.S., Yamani Z., Flacau R., Reuvekamp P. G., Schulz A., and Kremer R.K. (2016), *Phys. Rev*.B. **93**, 104414 .

27. Kaul S.N. and Siruguri V. (1992), *Journal of Physics*: Condensed Matter, **4**, 505.

28. Kaul S.N. and Siruguri V. (1987), *Journal of Physics* F: Met. Phys., **17**, L255.

Notes

Synthesis: Homogeneous single phase $EuCrO_3$ nanoparticles have been synthesized using a sol-gel followed by hydrothermal method. In the present case, the stoichiometric amounts of chromium nitrate ($Cr(NO_3)_3.9H_2O$ (Alfa-aesar, 99.9%), europium nitrate hydrate $Eu(NO_3)_3.3H_2O$, (Alfa-aesar, 99.9%), and citric acid (Merck, 99.5%) with 1:1:1 molar ratio were dissolved in the deionized water so that the metal ions can be completely complexed to the citrate ions. This was followed by the drop-wise addition of ammonia solution (25 wt %) to raise the pH value of the solution to reach 9-10 resulting in a sol formation. The sol was transferred to a 200 ml capacity autoclave with the Teflon liner and was subjected to hydrothermal treatment at 473 K for 24 h. The precipitate was, in turn, filtered, washed with deionized water and dried at 423 K for 24 h. A pellet of the as-synthesized powder was annealed at 973 K in air for 12 h to obtain $EuCrO_3$ nanoparticles.

EPR Measurements: Temperature dependent electron paramagnetic resonance (EPR) spectra were recorded in the X-band region on JEOL-FE3X ESR spectrometer in the range 123 – 373 K, using a liquid nitrogen (LN2) cryostat, at a fixed microwave frequency of about 9.2 GHz. The sample temperature was varied between 123 – 373 K by regulating the flow of cold nitrogen gas. A proper gas flow was achieved by controlling the power input to a heater, immersed in a liquid-nitrogen (LN2) container, with the aid of a proportional, integral and derivative (PID) temperature controller. The controlling sensor used was a pre-calibrated copper-constantan thermocouple situated just outside the microwave cavity. The temperature at the sample site was monitored by another pre-calibrated copper-constantan thermocouple in close contact with the sample. The temperature stability achieved at the sample site was within ±50 mK. The sample temperature was varied from 300 – 373 K by heating air blown through the cavity by a compressor. EPR spectrum has been recorded on empty EPR quartz tube along with thermocouple to check the presence and/or absence of any magnetic impurities of such combination.

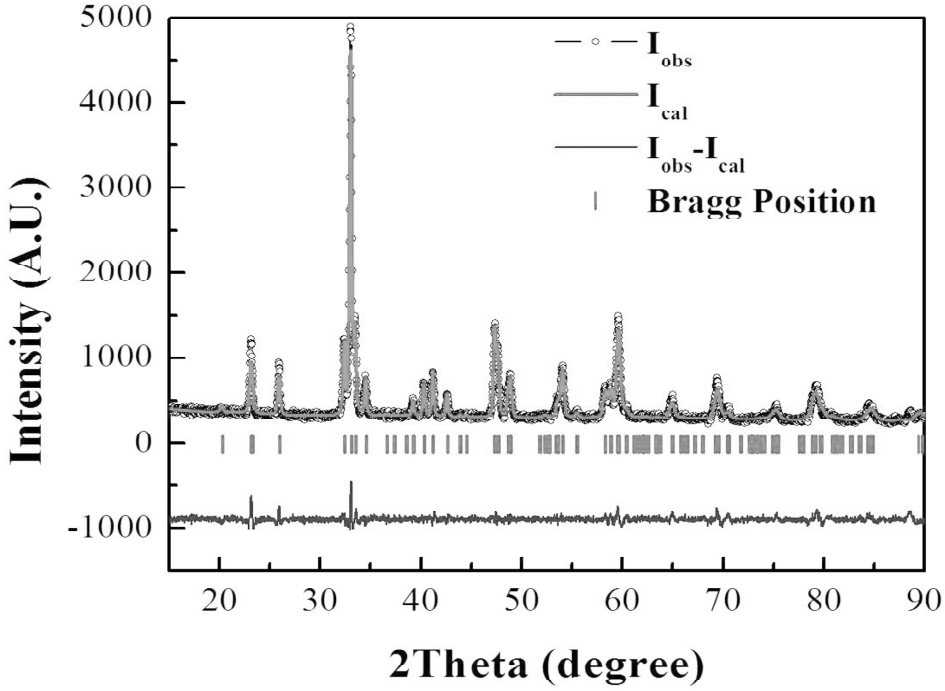

Figure 1 : Profile matching of the powder X-ray diffractogram of $EuCrO_3$ nanoparticles.

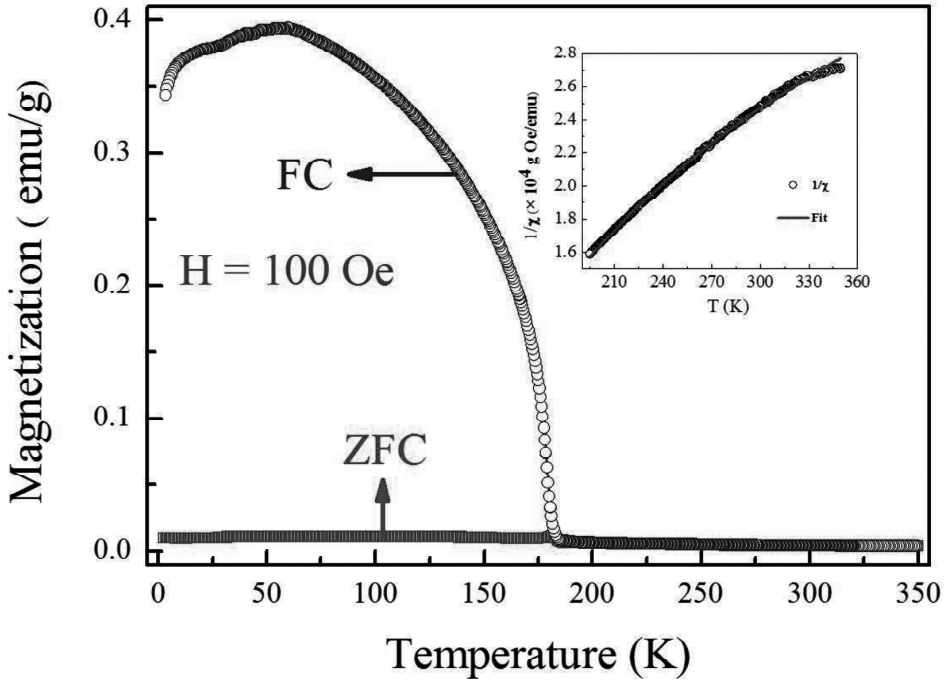

Figure 2 : Zero-field-cooled (ZFC) and Field-cooled (FC) magnetization of $EuCrO_3$ with temperature. The inverse susceptibility is shown in the inset.

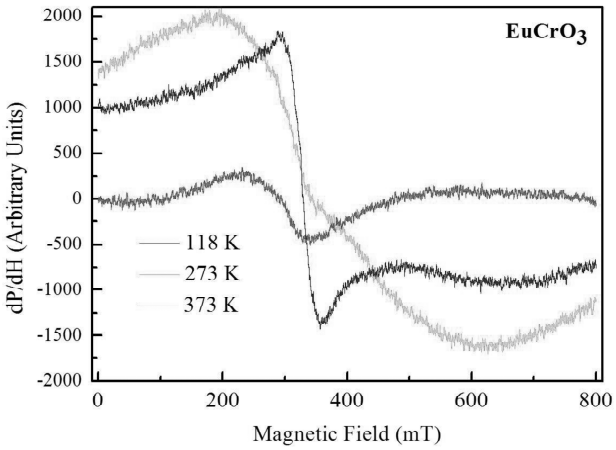

Figure 3 : The as-recorded EPR spectra of $EuCrO_3$ nanoparticles recorded at 118, 273 and 373 K.

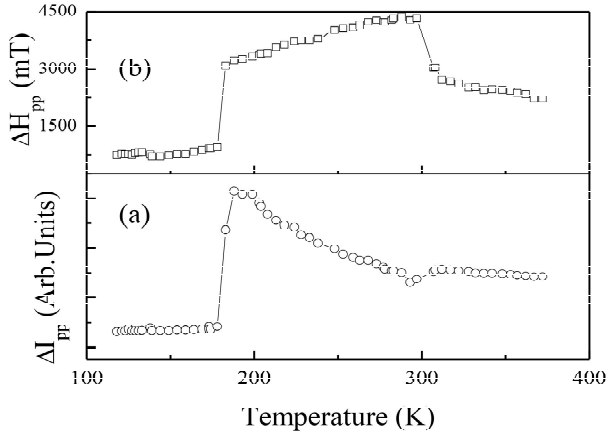

Figure 4 : The EPR spectral parameters peak-to-peak width (ΔH_{pp}) and differential intensity (ΔI_{pp}) of $EuCrO_3$ with temperature.

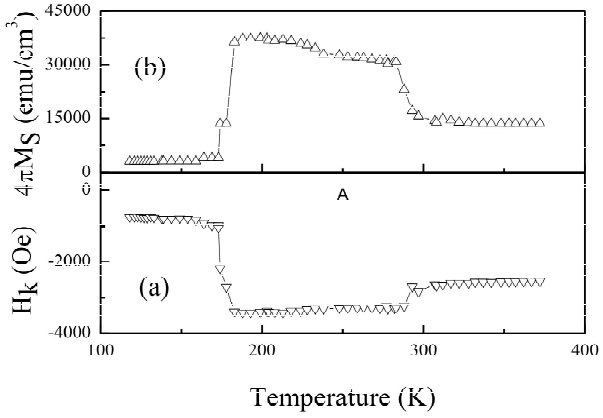

Figure 5 : The magnetic parameters spontaneous magnetization ($4\pi M_s$) and magnetic anisotropy field (H_k) of $EuCrO_3$ as a function of temperature.